

Daily maximum and minimum temperature trends in a climate model

Dáithí A. Stone and Andrew J. Weaver

School of Earth and Ocean Sciences, University of Victoria, Victoria, BC, Canada

Received 11 December 2001; revised 13 March 2002; accepted 14 March 2002; published 15 May 2002.

[1] The recent observed global warming trend over land has been characterised by a faster warming at night, leading to a considerable decrease in the diurnal temperature range (DTR). Analysis of simulations of a climate model including observed increases in greenhouse gases and sulphate aerosols reveals a similar trend in the DTR of -0.2°C per century, albeit of smaller magnitude than the observed -0.8°C per century. This trend in the model simulations is related to changes in cloud cover and soil moisture. These results indicate that the observed decrease in the DTR could be a signal of anthropogenic forcing of recent climate change. *INDEX TERMS*: 1610 Global Change: Atmosphere (0315, 0325); 1620 Global Change: Climate dynamics (3309); 3309 Meteorology and Atmospheric Dynamics: Climatology (1620); 3322 Meteorology and Atmospheric Dynamics: Land/atmosphere interactions

1. Introduction

[2] The mean surface air temperature over land areas increased at a rate of about 0.9°C per century over the 1950–1993 period [IPCC, 2001]. Three dimensional models of the climate system produce a comparable warming when they include the effects of increases in greenhouse gases and sulphate aerosols arising from human activities [Stott *et al.*, 2000; IPCC, 2001]. Analysis of station measurements indicates that the observed warming results largely from a general rise in daily minimum temperatures (T_{min}), with the increase in the daily maximum (T_{max}) being only about half as large [Easterling *et al.*, 1997]. The trend in the diurnal temperature range (DTR - the difference between T_{max} and T_{min}) amounts to -0.8°C per century, comparable to the mean warming itself. This differential temperature trend is a distinct characteristic of recent climate change, and could thus serve as a “fingerprint” for the identification of the natural and anthropogenic causes of the overall warming. However, despite the strength of this signal, its underlying cause and its relation to anthropogenic emissions remain poorly understood.

[3] Observational studies suggest that regions where the DTR has decreased have also tended to experience an increase in low base clouds [Karl *et al.*, 1993; Dai *et al.*, 1997, 1999]. The reflection of sunlight by these low level clouds would be expected to cause a drop in daytime temperatures, and indeed modelling studies indicate that the DTR would be quite sensitive to changes in cloud cover [Stenchikov and Robock, 1995; Dai *et al.*, 2001]. Thus increasing cloud coverage is suggested as the primary cause of the observed DTR decrease. However, increases in soil moisture, through control of evaporation and the ground heat capacity, as well as in sulphate aerosols, by scattering sunlight back to space, could also strongly influence the DTR. Moreover, due to difficulties in the availability and accuracy of measurements, observational verification for these relations is difficult, and thus model investigations are required.

[4] Studies with global climate models project a decrease in the DTR under enhanced greenhouse forcing [Cao *et al.*, 1992; Colman *et al.*, 1995; Mitchell *et al.*, 1995; Stenchikov and Robock, 1995; Reader and Boer, 1998; Dai *et al.*, 2001]. These investigations indicate that the DTR is relatively insensitive to short wave scattering by sulphate aerosols, but is influenced by clouds and soil moisture, as well as plant physiological responses [Collatz *et al.*, 2000]. In this paper, we evaluate the observed DTR trend as a potential signal of anthropogenic forcing by directly comparing simulations of a global climate model with observations, and relate the DTR trend to trends in other variables describing the climate system.

2. Methods

[5] This investigation uses simulations from the Canadian Centre for Climate Modelling and Analysis global climate model, CGCM1 [McFarlane *et al.*, 1992; Boer *et al.*, 2000; Flato *et al.*, 2000]. The atmospheric component of CGCM1 is a spectral model with an equivalent horizontal resolution of 3.75° and 10 unequally spaced vertical levels. The oceanic component is a grid point model of 1.875° horizontal resolution with 29 unequally spaced vertical levels. A thermodynamic sea ice module, and a single layer bucket model for energy and moisture at the land surface, form the other components of the model. We use an ensemble of three simulations (GHG+A1, 2, 3) which include observed increases in greenhouse gases as well as the scattering of sunlight by increases in sulphate aerosols over the 1950–1993 period [Reader and Boer, 1998]. The aerosols are represented through changes in the surface albedo. These three simulations are taken from three larger 1900–2100 integrations of CGCM1, which are identical except for their initial conditions, and so represent independent possible realisations of recent climate.

[6] A more recent version of the CCCma model (CGCM2) uses different parametrisations to represent ocean mixing and sea ice [Flato and Boer, 2001]. In particular, the Gent and McWilliams parametrisation for mixing associated with mesoscale eddies [Gent and McWilliams, 1990] and a cavitating fluid representation of sea ice [Flato and Hibler, 1992] are included. Three simulations of this model including the observed changes in greenhouse gases and sulphate aerosols are also examined. The primary difference from the GHG+A simulations of CGCM1 is a much larger warming in the southern high latitudes.

3. Results

[7] We first compare annual mean trends in the DTR from the model simulations with those from the observations. Values from the model grid are interpolated to the observational grid, and retained only where observational measurements exist [Easterling *et al.*, 1997]. The model trend in (T_{max}) ranges from 1.3 to 1.5°C per century (Figure 1). We use a 201 year simulation of the model with constant natural forcing (CTRL) to estimate the range of 44 year trends plausible due to random natural variability. With this estimate of the natural variability, we find that the trend in annual mean T_{max} in the model simulations is significantly

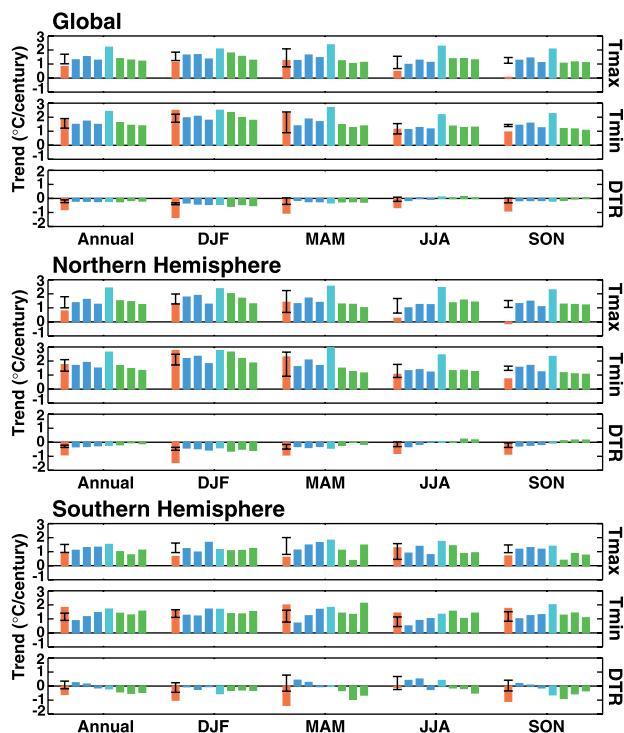


Figure 1. 1950–1993 seasonal trends in T_{max} , T_{min} , and the DTR. Global and hemispheric trends are shown. The red values are the observed trends at nonurban stations in *Easterling et al.* [1997]; values from the three GHG+A model simulations are in dark blue, while those from the GHG simulation are in light blue. The values in green are from simulations including both greenhouse gases and sulphate aerosols using a newer version of the CCCma model. The error bars denote the 95% confidence interval of the GHG+A simulations, calculated from the natural variability of the CTRL simulation. DJF is the December–February season, MAM is March–May, JJA is June–August, and SON is September–November.

higher than the 0.8°C per century inferred from observational measurements (at the 5% level for a two-sided test). On the other hand, the increases in (T_{min}), ranging from 1.5 to 1.7°C per century, are consistent with the observed warming of 1.8°C per century. In both cases the trends are significantly different from zero change. As with the observations, these differential temperature trends in the model integrations result in a significant decrease in the DTR (Figure 2). However, this change of -0.2°C per century is considerably, and significantly, smaller than the observed -0.8°C per century.

[8] In the Northern Hemisphere, decreases occur in the DTR in all seasons in the model simulations, with those during autumn, winter, and spring being statistically significant (Figure 1). The modelled trends tend to be largest in the winter, as is the case in the observations. In all seasons, however, the model underestimates the observed trends. During winter and spring the modelled and observed trends in T_{max} agree well with each other. The increases in T_{min} , on the other hand, tend to be smaller in the model, and this results in the smaller decrease in the DTR. The opposite is the case during the summer and autumn, in which case the DTR trends are underestimated in the model due mainly to an overestimate of the warming in T_{max} . Possible reasons for this seasonal pattern are discussed below.

[9] Unlike in the Northern Hemisphere, the seasonal and annual DTR trends in the Southern Hemisphere in the model simulations are not significantly different from zero. With the exception of

winter, these changes are considerably smaller than the observed values. As is the case for the Northern Hemisphere, the underestimation results primarily from an overestimation of the T_{max} warming during the summer and autumn, and an underestimation of the T_{min} warming during the spring. The large spread of trend estimates between the model simulations indicates that the size of the station network in the Southern Hemisphere is as yet insufficient to robustly estimate the DTR trends. In fact, trends calculated for all Southern Hemisphere land areas (excluding Antarctica) are systematically less negative in the simulations. However, this sampling effect of about $\pm 0.3^{\circ}\text{C}$ per century is not large enough to affect the sign of the observed -0.6°C per century decrease.

[10] The global warming simulations of CGCM2 predict T_{max} , T_{min} , and DTR trends in the Northern Hemisphere similar to those in the GHG+A simulations of CGCM1 (Figure 1). Since most of the land in this hemisphere is far away from the ocean, it is not surprising that a different ocean component for the model has no obvious effect on the DTR over land. However, ocean dominates over land in the Southern Hemisphere, so most land is in relative close proximity to the ocean. Indeed, the DTR tends to decrease more in these simulations than in those from CGCM1, and they more closely resemble the observations. This better agreement arises from improved prediction of both the T_{max} and T_{min} trends, and demonstrates that better representation of high latitude ocean and sea ice processes is necessary to properly represent Southern Hemisphere climate, even over land areas.

[11] Observed changes in the DTR are not uniform. For instance, increases have actually occurred over northeast Canada and the South Pacific islands (Figure 3). Similar regional increases also occur in the model simulations, but the patterns do not resemble that observed. However, the regional changes in the different simulations are also rather different from one another. For instance, in one simulation the DTR decreases uniformly over Australia, while in another it increases and in the third remains fairly constant. This indicates that regional trends in the DTR may not be distinguishable from random natural variability over the rather short 1950–1993 period.

[12] The most notable difference between the spatial pattern of the DTR trend between the model simulations and the observations is over island areas, especially in the South Pacific Ocean. This discrepancy arises from differences in the representation of these areas. Observational measurements come from land stations, and thus are biased toward the small islands. On the other hand, since there is more water than land in these grid boxes they are represented as ocean in the model. The DTR over the sea is considerably smaller than over land due to the large thermal capacity of water. Consequently, long term trends would also be smaller over water than on land, and most likely not even detectable at this stage. However, removal of these island areas from the comparison amounts to only a further 0.05°C per century decrease in the DTR.

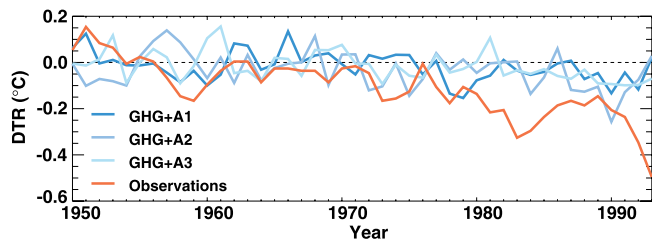
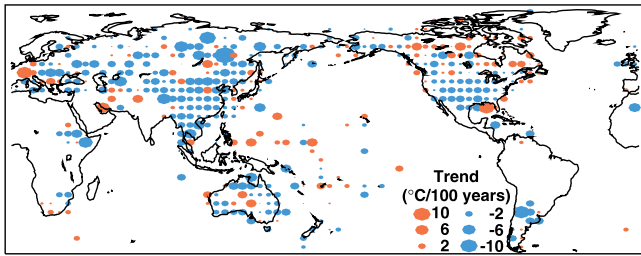
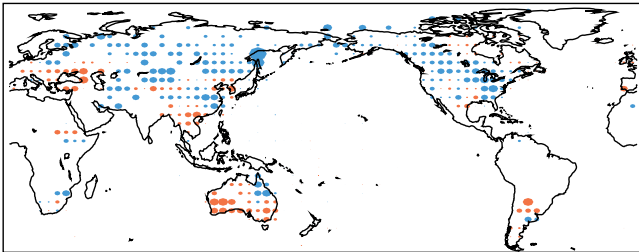


Figure 2. 1950–1993 time series of annual mean DTR. The time series from nonurban station measurements, from *Easterling et al.* [1997], is in red, while the blue lines represent the time series from the three GHG+A model simulations. Values are anomalies from the 1950–1959 mean.

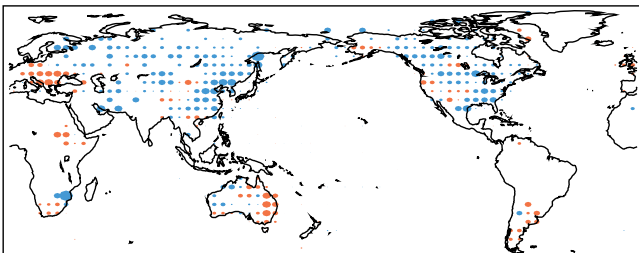
Observations



GHG+A1



GHG+A2



GHG+A3

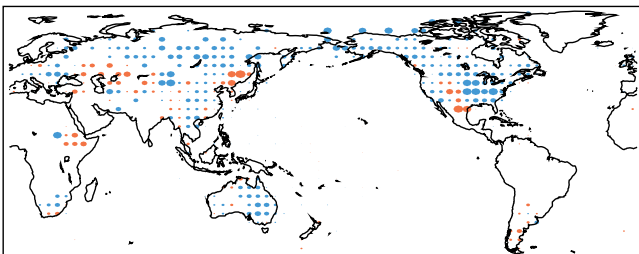


Figure 3. 1950–1993 DTR trends in the observations and the three GHG+A model simulations for each 5° by 5° grid box. The observations are from *Easterling et al.* [1997] and are calculated from nonurban stations. The scale is identical for all maps.

[13] The scattering of sunlight by increasing concentrations of sulphate aerosols could be a cause of the DTR decrease, since this diminishes the amount of energy reaching the surface during the daytime. However, results from a simulation of the model omitting increases in aerosol concentrations, but still including those in greenhouse gases (GHG), indicate that this is not the case (Figure 1). While the warming of T_{min} and T_{max} is much larger in this GHG simulation, changes in the DTR are similar to those in the GHG+A simulations in most seasons. Thus in the model simulations the DTR decrease is a result of the increase in greenhouse gases and is largely independent of the emission of sulphate aerosols, as found in other spatial-temporal domains [Reader and Boer, 1998; Stone and Weaver, 2002] and other models [Cao et al., 1992; Mitchell et al., 1995; Stenchikov and Robock, 1995]. *Stenchikov and Robock* [1995] suggest that the effect of aerosol scattering on the DTR is cancelled by a water vapour feedback. In the cooler climate resulting from the aerosols, less atmospheric water vapour is present to absorb near-infrared

solar radiation, thus increasing the total radiation reaching the surface.

[14] Other suggested influences on the DTR trend are increases in cloud cover and soil moisture. During the daytime clouds reduce the amount of sunlight reaching Earth's surface. Increases in soil moisture permit faster cooling during the daytime through evaporation and also moderate temperatures by increasing the heat capacity of the ground. Our analysis suggests that changes in these two factors are indeed related to the DTR trend in the model simulations. We create a multiple regression model of the effects of changes in daytime cloud cover and soil moisture on the DTR using the 201 years of the CTRL simulation. Daytime cloud cover is measured here by the amount of solar radiation reaching the ground. We input variations in these two factors in the climate change simulations into the regression model to estimate the changes in the DTR. The correlation between the estimated and actual DTR time variations for the GHG+A1 simulation is 0.91 over the 1950–2100 period, while their trends are both -0.22°C per century (Figure 4). Use of only one of these variables to predict the DTR results in considerably less accurate correspondences, indicating that both are important. A more detailed spatio-temporal analysis in *Stone and Weaver* [2002] further supports this result, as do previous modelling studies [*Stenchikov and Robock*, 1995; *Collatz et al.*, 2000; *Dai et al.*, 2001]. Interestingly, variations and changes in the mean temperature and DTR are rather unrelated (not shown).

[15] The influence of soil moisture on the DTR arises through a number of mechanisms. Variations in soil moisture are caused by changes in evaporation and precipitation, both of which are related to cloud cover. Thus the relations between soil moisture and the DTR could simply reflect the correlation of both to cloud cover. However, removal of the component of the soil moisture variations correlated with cloud cover reveals that the residual still has an important relation to the DTR variations and trend. Another possibility is that soil moisture influences the DTR through changes in evaporation and vegetative evapotranspiration [*Collatz et al.*, 2000]. However, in the model simulations this effect is largely cancelled by opposite changes in the sensible heat flux. The possibility that soil moisture acts as a proxy for the water vapour radiative feedback described by *Stenchikov and Robock* [1995] is not supported by the lack of covariation between specific humidity and the DTR (not shown). This leaves changes in the moderating effect of the heat capacity of the ground as the main mechanism relating soil moisture to the DTR decrease in the model. Of course, the importance of this mechanism may be magnified by the use in CGCM1 of the single layer bucket model in representing the land surface.

[16] The reflection of incoming solar radiation by cloud cover serves to reduce T_{max} , leaving T_{min} relatively unaffected. Thus underestimates of daytime increases in cloud cover in the GHG+A1 simulations would result in the overestimate of T_{max} during summer, as noted earlier. During this season the amplitude

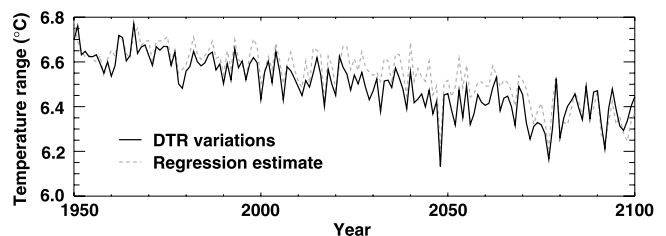


Figure 4. Time series of annual mean DTR from 1950 through 2100 in the GHG+A1 simulation. The solid line is the actual value from the simulation, while the dotted line is estimated using a regression model from variations in daytime cloud cover and in soil moisture.

of the diurnal cycle of solar radiation is highest, and so T_{max} would be most sensitive to the reflection of sunlight by clouds. During the winter, on the other hand, the presence of snow both reflects much of the incoming sunlight and insulates the atmosphere from the soil moisture. The importance of clouds during this season lies in their downward emission of infrared radiation, which serves to maintain temperatures overnight. Therefore, an underestimate of increasing cloud cover during the winter would result in an underestimate of the T_{min} trend, such as occurs in the GHG+A simulations. The importance of cloud cover to the DTR is evidenced by the CGCM2 simulations. These simulations and the GHG+A simulations of CGCM1 differ mainly in that the former predict a much larger warming of the surface ocean and atmosphere in the Southern Hemisphere as a consequence of an improved representation of ocean mixing. A warmer atmosphere over a warmer ocean implies more moisture in the air, which then forms clouds when passing over land. Indeed, cloud cover increases substantially in the Southern Hemisphere in the CGCM2 simulations, producing better agreement with the observed temperature trends. Therefore, an underestimate of an increase in global cloud cover over land in the model simulations could account for much of the discrepancy between the modelled and observed trends in the DTR.

[17] Forced with predicted changes in greenhouse gases and sulphate aerosols CGCM1 projects a continued decrease in the DTR through the twenty-first century (Figure 4). During the December–February and March–May seasons the DTR is projected to decrease at a similar rate as in the 1950–1993 period. On the other hand, little change is projected to occur during the June–August and September–November seasons. Due to the spatial bias of the stations, this pattern of change is dominated by large decreases in the Northern Hemisphere during the winter and spring.

4. Conclusion

[18] These results indicate that the observed decreases in the DTR could be a climatic response to anthropogenic emissions of greenhouse gases and aerosols. In particular, changes in cloud cover and soil moisture associated with climate change force the DTR reduction. However, a discrepancy in the magnitude of the trend between observations and the model simulations remains. The importance of soil moisture found here implies that physiological responses of vegetation to climate change could be quite important for the behaviour of the DTR. Improvements in the parametrisation of clouds and land surface processes are currently among the most actively pursued goals in climate model development. Thus more reliable estimates of the importance of the observed DTR trend as a fingerprint of anthropogenic forcing of climate change can be expected in the near future. At this early stage, however, model results are consistent with the observed DTR decrease over the last half century, and suggest that this trend is likely to continue into the foreseeable future.

[19] **Acknowledgments.** The authors wish to thank George Boer, David Easterling, Viatcheslav Kharin, and the Canadian Centre for Climate Modelling and Analysis for supplying the data used in this analysis, as well as two anonymous reviewers for many helpful comments and suggestions. Financial support for this research from the Climate Change Action Fund, the Meteorological Service of Canada/Canadian Institute for Climate Studies, the National Sciences and Engineering Research Council/Canadian

Foundation for Atmospheric Studies CLIVAR project, and the National Sciences and Engineering Research Council is gratefully acknowledged.

References

- Boer, G. J., G. M. Flato, M. C. Reader, and D. Ramsden, A transient climate change simulation with greenhouse gas and aerosol forcing: experimental design and comparison with the instrumental record for the twentieth century, *Clim. Dyn.*, 16, 405–425, 2000.
- Cao, H. X., J. F. B. Mitchell, and J. R. Lavery, Simulated diurnal range and variability of surface temperature in a global climate model for present and doubled CO₂ climates, *J. Climate*, 5, 920–943, 1992.
- Collatz, G. J., L. Bounoua, S. O. Los, D. A. Randall, I. Y. Fung, and P. J. Sellers, A mechanism for the influence of vegetation on the response of the diurnal temperature range to changing climate, *Geophys. Res. Lett.*, 27, 3381–3384, 2000.
- Colman, R. A., S. B. Power, B. J. McAvaney, and R. R. Dahni, A non-flux corrected transient CO₂ experiment using the BMRC coupled atmosphere/ocean GCM, *Geophys. Res. Lett.*, 22, 3047–3050, 1995.
- Dai, A., I. Y. Fung, and A. D. Del Genio, Surface observed global land precipitation variations during 1900–88, *J. Climate*, 10, 2943–2962, 1997.
- Dai, A., K. E. Trenberth, and T. R. Karl, Effects of clouds, soil moisture, precipitation, and water vapor on diurnal temperature range, *J. Climate*, 12, 2451–2473, 1999.
- Dai, A., T. M. L. Wigley, B. A. Boville, J. T. Kiehl, and L. E. Buja, Climate of the twentieth and twenty-first centuries simulated by the NCAR Climate System Model, *J. Climate*, 14, 485–519, 2001.
- Easterling, D. R., et al., Maximum and minimum temperature trends for the globe, *Science*, 277, 364–367, 1997.
- Flato, G. M., and G. J. Boer, Warming asymmetry in climate change simulations, *Geophys. Res. Lett.*, 28, 195–198, 2001.
- Flato, G. M., and W. D. Hibler III, Modelling pack ice as a cavitating fluid, *J. Phys. Oceanogr.*, 22, 626–651, 1992.
- Flato, G. M., G. J. Boer, W. G. Lee, N. A. McFarlane, D. Ramsden, M. C. Reader, and A. J. Weaver, The Canadian Centre for Climate Modelling and Analysis global coupled model and its climate, *Clim. Dyn.*, 16, 451–467, 2000.
- Gent, P. R., and J. C. McWilliams, Isopycnal mixing in ocean circulation models, *J. Phys. Oceanogr.*, 20, 150–155, 1990.
- IPCC, *Climate Change 2001: The Scientific Basis. Contribution of Working Group I to the Third Assessment Report of the Intergovernmental Panel on Climate Change*, Cambridge University Press, Cambridge, England, 2001, in press.
- Karl, T. R., et al., Asymmetric trends of daily maximum and minimum temperature, *Bull. Amer. Meteor. Soc.*, 74, 1007–1023, 1993.
- McFarlane, N. A., G. J. Boer, J.-P. Blanchet, and M. Lazare, The Canadian Climate Centre second-generation general circulation model and its equilibrium climate, *J. Climate*, 5, 1013–1044, 1992.
- Mitchell, J. F. B., R. A. Davis, W. J. Ingram, and C. A. Senior, On surface temperature, greenhouse gases, and aerosols: Models and observations, *J. Climate*, 8, 2364–2386, 1995.
- Reader, M. C., and G. J. Boer, The modification of greenhouse gas warming by the direct effect of sulphate aerosols, *Clim. Dyn.*, 14, 593–607, 1998.
- Stenchikov, G. L., and A. Robock, Diurnal asymmetry of climatic response to increased CO₂ and aerosols: Forcings and feedbacks, *J. Geophys. Res.*, 100, 26,211–26,227, 1995.
- Stone, D. A., and A. J. Weaver, Diurnal temperature range trends in 20th and 21st century simulations of the CCCma coupled model, *Clim. Dyn.*, 2002, submitted.
- Stott, P. A., S. F. B. Tett, G. S. Jones, M. R. Allen, J. F. B. Mitchell, and G. J. Jenkins, External control of 20th century temperature by natural and anthropogenic forcings, *Nature*, 290, 2133–2137, 2000.

D. A. Stone, School of Earth and Ocean Sciences, University of Victoria, P.O. Box 3055, Victoria, BC V8W 3P6, Canada. (stone@ocean.seos.uvic.ca)

A. J. Weaver, School of Earth and Ocean Sciences, University of Victoria, P.O. Box 3055, Victoria, BC, V8W 3P6, Canada. (weaver@uvic.ca)